Journal of Medical Diagnostic Methods
ISSN: 2168-9784

Kaneko et al., J Med Diagn Meth 2013, 2:6
DOI; 10.4172/2168-9784.1000145

Research Article Open Access

Low Density Regions of DNA in Human Sperm Appear as Vacuoles after Translucent Staining With Reactive Blue 2

Satrou Kaneko*, Joji Yoshida and Kiyoshi Takamatsu

Department of Obstetrics and Gynecology, Ichikawa General Hospital, Tokyo Dental College, Chiba, Japan

Abstract

Human sperm often contain vacuoles, and it is therefore necessary to determine whether vacuoles in the chromosomal region are responsible for DNA deterioration. To that end, the present study developed a novel clinical examination technique, translucent staining, for the visualization of vacuoles. Highly diluted Reactive Blue 2 (RB2, 100 pmol/L) faintly stained the sperm head to reveal a translucent bluish body with toneless spots. Differential interference contrast showed the vacuoles as shaded-relief images. In the same, field of view the localization and the shape of the toneless spots were coincided with the shaded-relief images.

Dual staining with RB2 and DNA fluorescent dye suggested that the vacuoles might include vacant or low-density DNA. The present results revealed important issues in clinical Assisted Reproductive Technology (ART), that is, a variety of vacuoles were involved regardless of the normalcy of outline or the motility. Features were classified into three categories: zero or one small vacuole; multiple sporadic vacuoles of various sizes; and one large vacuole. Moreover, in vitro processing steps such as density gradient centrifugation and subsequent swim up could not isolate sperm without vacuoles.

Since it is still unknown whether the vacuoles merely push out DNA to the surroundings without damaging it, or if the empty region is a consequence of DNA degradation, the translucent staining for simultaneous visualization of the outline and vacuoles constitutes a major step for pre-ART cyto-diagnosis to determine whether the sperm population is competent for use in clinical ICSI.

Keywords: Human sperm; Vacuole; Translucent stain; Reactive blue 2; MSOME; IMSI

Introduction

In 1978, the first human baby was born through *in vitro* fertilization-embryo transfer. To date, more than a million children have already been born with the help of Assisted Reproductive Technology (ART). Fertilization through Intracytoplasmic Sperm Injection (ICSI) now accounts for more than half of clinical ART cases worldwide [1]. Males with infertility due to dysfunction of spermatogenesis are the primary candidates for ICSI. The technique for sperm injection has been fully established and reported in detail; however, the selection of sperm depends on intraoperative assessment. It is based on observations of sperm motility and gross morphology as obtained using an inverted microscope equipped with Hoffman modulation contrast optics or Differential Interference Contrast (DIC) optics. Human ejaculate contains a heterogeneous sperm population with a variety of abnormalities. Numerous literatures reported that the rate of DNA-damaged sperm increased in male infertility with poor semen quality [2-5]. If the oocyte incorporates with a sperm with damaged DNA, this may lead to sperm-derived chromosomal aberrations. Several recent cohort studies reported that the rate of birth defects in babies conceived through ART, especially through ICSI, were found to be higher than the rate in natural births [6-8]. There are no validated methods to address and assure DNA integrity of sperm.

Human sperm head has organelles that may observed via electron microscopy as nuclear vacuoles or hollows at the cell surface [9]. Several authors proposed a Motile Sperm Organelle Morphology Examination (MSOME) to evaluate human sperm using DIC optics at high magnification (6000×) through additional digital zooming [10-12]. When compared Intra-Cytoplasmic Morphologically Selected Sperm Injection (IMSI) that evaluated the sperm normality based on MSOME with conventional ICSI, IMSI has brought improved developmental rate of embryo to the blastocyst stage as well as implantation and pregnancy rates [10,13,14].

In terms of sperm quality control in ART, it is important to determine whether the organelles present in the chromosomal area are associated with DNA deterioration and potentially consequent infant abnormalities. Since human sperm head and its organelles are transparent, the present study developed a novel translucent staining method using Reactive Blue 2 (RB2) as a first step to observe simultaneously sperm morphology and the organelles under bright field optics [15-19].

Methods

Ejaculates were obtained from volunteers or patients who visited our clinic. All study participants who provided the ejaculates received explanations on the aim of this study, and then gave written consent. The ethical committee of Ichikawa General Hospital specifically approved this study. The sperm parameters (concentration, motility, and morphology) were observed in accordance with the guidelines of the World Health Organization (WHO) Laboratory Manual [20].

***Corresponding author:** Satrou Kaneko, Department of Obstetrics and Gynecology, Ichikawa General Hospital, Tokyo Dental College, 5-11-13 Sugano, Ichikawa, Chiba 272-8513, Japan, Tel: 080-473-22-0151; Fax: 080-473-22-8931; E-mail: kaneko@tdc.ac.jp

Received September 17, 2013; **Accepted** November 23, 2013; **Published** November 25, 2013

Citation: Kaneko S, Yoshida J, Takamatsu K (2013) Low Density Regions of DNA in Human Sperm Appear as Vacuoles after Translucent Staining With Reactive Blue 2. J Med Diagn Meth 2: 145. doi: 10.4172/2168-9784.1000145

Sperm with progressive motility were prepared according to our previous reports [21,22]. Briefly, the ejaculate was diluted several times with 20 mM HEPES-buffered Hanks' solution and 10 mg/mL human serum albumin (pH 7.4), and then centrifuged in a density gradient of 90% Percoll. The motile sperm was separated by the swim-up method. Hanks' solution (1.0 ml) was layered on the sediment (0.2 ml) and was allowed to stand for 60 min at ambient temperature. Motile sperm that swam up into the upper half of the medium was recovered.

Rapid May–Giemsa staining (Diff-Quik; Siemens, IL, USA) was performed as described previously [23]. Translucent staining was carried out as follows: A suspension containing 10^5 human sperm cells was diluted with saline to yield a 2.0 mL volume, which was layered on a conical bottom tube containing 2.0 mL of 100 pmol/L RB2 (1-amino-4-[[4-[[4-chloro-6-[[3(or4)-sulfophenyl]amino-]-1,3,5-triazin-2-yl]amino]-3-sulfophenyl]amino]-9,10-dihydro-9,10-dioxo-2-anthracensulfonic acid; Alexis Biochemical, CA, USA) and a 0.05% Triton X-100 solution in 1.0 M sucrose. Sperm passing through the dye layer were collected in the sediment by centrifugation at 600×g for 10 min in a swing-out rotor. A smear was prepared by using a centrifugal automatic smear machine (Sakura Finetek, Tokyo, Japan). Sperm adhering to an amino-propyl silane coupling glass slide was mounted with 10 µL of 1.0 M sucrose in water, and was covered with a cover slip. Specimens were observed under oil immersion using a transmitted light upright microscope (Axio Imager A1; Carl Zeiss Microimaging, Germany, Jena) with bright field (630×, 1000×). The same apparatus with an appended DIC optical system recorded DIC images. Still images were recorded using a high-resolution charge-coupled device camera (4164 × 3120 pixels, AxioCam HRC; Carl Zeiss Microimaging), and displayed on a large, full hi-vision digital display (1920 × 1080 pixels) with the help of AxioVision software (Revision 4.7.2; Carl Zeiss Microimaging). The original images were unnecessarily large; hence, unless otherwise stated, images were zoomed out to less than 50%. The morphology of the sperm was determined in accordance with the guidelines of the WHO Laboratory Manual, and the vacuoles were classified into three categories according to their size; large, medium, and small [20].

DNA in the head of the sperm was stained with diluted ($\times 10^5$) Cyber-Gold (Molecular Probes, Oregon, USA), and then observed under an epifluorescent microscope (excitation: 495 nm, emission: 537 nm).

To visualize the acrosome, sperm stained with RB2 was further labeled with 20 µg/mL Alexa 488-conjugated concanavalinA (Invitrogen, CA, USA), 3.0 mM methyl α-D-mannopyranoside in 20 mM MES buffered Hanks' solution (pH 6.0) for 30 min [24]. The excess dye was washed out with saline, and the specimen was observed under an epifluorescent microscope (excitation: 495 nm, emission: 537 nm). The bar at lower right of the figures represents 10 µm.

Results

Virtual shading by DIC optics visualized a variety of shaded-relief images in the heads; in MSOME these organelles are termed as vacuoles (Figure 1A) [10-12]. Figure 1 shows a typical motile sperm fraction with normal head morphology, with the majority containing shaded-relief images in the heads. The number, size, and shape varied significantly between individual sperm. In the same field of view, sperm stained with RB2 through the objective lens were visual as faintly bluish stained cells, while the image capture device recorded clear images of bluish stained cells with the hollows appearing as toneless spots (Figure 1B). The localization and shape of the toneless spots detected by the novel method and the shaded-relief images by DIC corresponded with each other.

When the same specimen was observed by the commonly used rapid May–Giemsa staining, high-contrast images of the sperm were obtained with crisp outlines, the toneless spots were concealed since they were deeply stained (Figure 1C). The original image of the RB2-stained sperm was unnecessarily large for observation of the organelles, demonstrating that the use of additional digital zooming was expendable (Figure 1D).

The state of the DNA in the toneless spots was estimated by dual staining with RB2 and Cyber-Gold. In Figures 2A and 2B depicts a comparison of the same field of view. The localization and shape of the toneless spots corresponded with the regions of fluorescent intensity lower than those of surrounding. Figures 2C and 2D also show a comparison of the same field of view to observe the positional relationship between the acrosome and the toneless spots. Since the detergent removed the plasma membrane during RB2 staining, the fluorescence at the anterior portion of the heads derived from the acrosome at the first surface. Even observed the toneless spots in the acrosomal region, the fluorescence was smooth except one sperm indicated by the arrow; it gave anun level image corresponding to the shape of toneless spots. These results suggested that DNA might be vacant or be present at low-density in the toneless spots, and that nearly all of it may be located at the underside of the acrosome but not in the hollows at the cell surface. We therefore deduced that almost all of the toneless spots are indicative of the vacuoles inside the cells. It is still unclear whether DNA was pushed out to the surrounding area without being damaged, or the empty region was a consequence of DNA degradation.

The frequency and features of the vacuoles varied widely among the ejaculates as well as the motile sperm fraction. Figures 3 and 4 summarize four typical specimens. Both ejaculates in Figures 3A and 3C are present normozoospermia, and Figures 3B and 3D show the

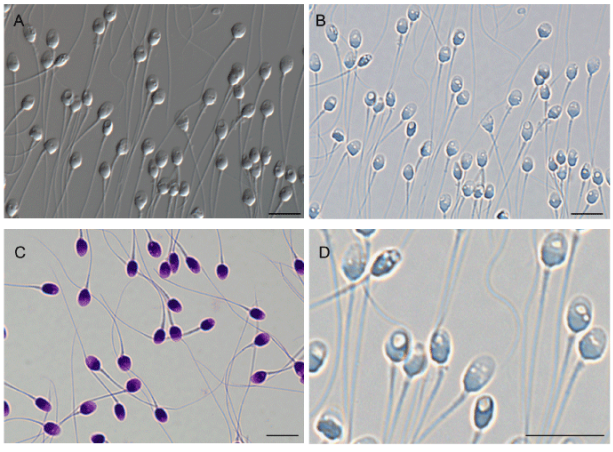

Figure 1: Comparison of sperm images visualized by DIC, translucent staining, and Diff-Quik staining

Sperm parameters in the ejaculate and those after the swim-up were as follows: sperm concentration: 86/0.66× 106 sperm/mL, motility: 54/97%, and normal morphology: 17/32%. All photographs show sperm in the swim-up fraction. (A): DIC image, (B): translucent stain, (C): Diff-Quik stain, and (D): original-size image of the translucent stain.

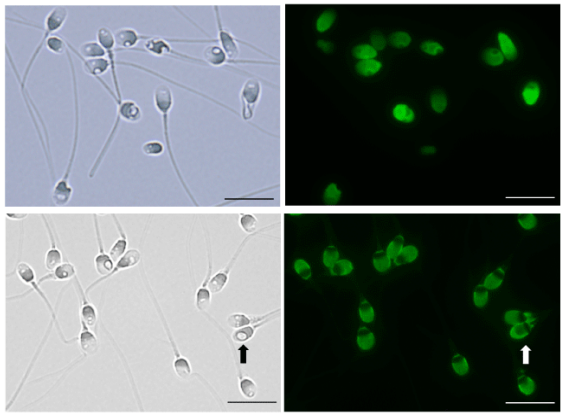

Figure 2: The state of DNA in the toneless spots and the positional relationship between the acrosome and the toneless spots.

Sperm parameters in the ejaculate and those after the swim-up were as follows: sperm concentration: 54/0.94×10^6 sperm/mL, motility: 62/95%, and normal morphology: 9.4/18%. All photographs show sperm in the swim-up fraction.

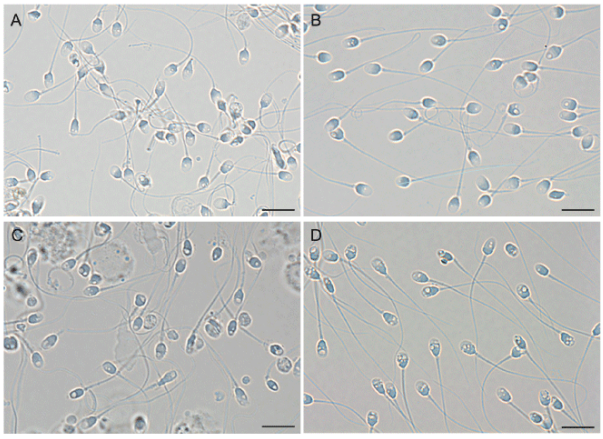

Figure 3: Simultaneous observation of morphology and vacuoles in normozoospermia specimens. Comparison of ejaculate and swim-up fraction

Sperm concentration, motility, and normal morphology: (A): 120×10^6/mL, 67% and 21%; (B): 26×10^6/mL, 95% and 32%; (C): 87×10^6/mL, 71% and 11%; (D): 9.0×10^6/mL, 92% and 18%.

motile sperm fraction prepared from specimens A and C, respectively. A majority of the sperm had oval heads with small vacuoles; in contrast, more than half of the sperm in Figure 3C also had oval heads, and almost all of them contained a variety of vacuoles (Figure 3A). After the swim-up, the percentage motilities were found to be >90% in both specimens despite large differences between them interms of frequency of vacuoles. The sperm in Figure 3B contained no vacuole or one small vacuole, whereas almost all sperm in Figure 3D contained vacuoles of various shapes. Figure 4 shows the specimens indicative of terato-asthenozoospermia and oligo-terato-asthenozoospermia (Figures 4A and 4C). Both specimens had extremely low motility and possessed few sperm with normal morphology; furthermore, almost all sperm contained vacuoles. After the swim-up, few sperm from the terato-asthenozoospermia specimen moved to the upper half of the medium. The lower half of the medium was also recovered, but the percentage motility remained at 44%. Although less than half of the sperm cells were immotile, almost all of them showed abnormal outlines with vacuoles of varying number and shape (Figure 4B). In the oligo-terato-as the no zoospermia specimen, no sperm were recovered in the swim-up fraction because of their poor motility.

As shown in Figure 5, the features of vacuole were classified into three categories; (A) zero or one small vacuole, (B) multiple sporadic vacuoles of various sizes, and (C) one large vacuole. The left and right columns in the figure compare the oval heads in the motile sperm fractions shown in Figures 3B and 3D, and amorphous heads in Figures 4A-4C, respectively. The features of the vacuoles varied among individual sperm, and their frequency of appearance differed among ejaculates. Notably, *in vitro* processing to separate motile sperm could not isolate those without vacuoles. We propose the formula A/(A+B+C) × 100 to evaluate the percentage of vacuole-negative sperm. This formula could accurately determine separated motile sperm with the oval heads (image A in the left column). When all the sperm is assumed motile, for example, the values in Figures 3B and 3D are approximately 86% and 8.2%, respectively. In contrast, this formula could not be applied to the sperm in Figure 4, because almost of them did not meet the other requirements.

Discussion

The morphology of the human sperm head has been recognized as one of the important parameters for the prediction of the outcome of conventional *in vitro* fertilization as well as ICSI [20,23,25]. WHO recommends Papanicolaou or rapid May–Giemsa staining methods to observe human sperm morphology [23,26]. The normality of sperm outlines were determined according to the strict criteria proposed by Kruger et al. [27]. The vacuoles were however, concealed because of the deep color of the high-contrast dye (Figure 1C).

Several years ago, we investigated ATP-activated channels in human sperm and examined the pharmacological actions of various antagonists. RB2,a well-known highly potent P2Y purine-receptor antagonist, is bluish at a high concentration [15,16]. We found that incubation of human sperm with RB2at the pharmacological dosage (in the order of pmol/L), which rendered the solution clear; however, the agent weakly stained the sperm to a translucent bluish color with toneless spots. In biochemical studies, RB2 is used in dye-ligand affinity chromatography of serum albumin and some dehydrogenases, which require NAD as the coenzyme. Since the adsorption of this agent is limited to a small fraction of proteins in human sperm, they appear as translucent bluish bodies but the vacuoles remain transparent [17-19]. If the specimens are contaminated with proteins, such as albumin derived from seminal plasma or the culture medium, adsorption of the agent to the sperm is suppressed competitively. Therefore, we developed a centrifugal staining method to facilitate the simultaneous removal of proteins, staining of sperm, and concentration of sperm in the sediment.

Virtual shading by DIC gave a three-dimensional appearance to cells, whereas the tone varied significantly with modulation of optical components such as the prism and polarizer. This is rather inconvenient in the context of clinical examinations. MSOME was characterized by the enlarged images up to 6000×magnification by additional digital zooming, the data processing, however, deteriorated the graphic resolution due to the reduced number of pixels. In contrast, the translucent staining with RB2 provided sufficient graphic resolution

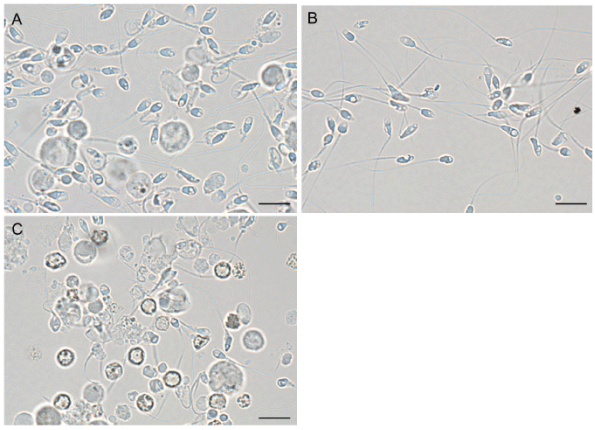

Figure 4: Simultaneous observation of morphology and vacuoles in terato-asthenozoospermia and oligo-terato-asthenozoospermia specimens: comparison of ejaculate and swim-up fraction Sperm concentration, sperm motility, and normal morphology: (A): 5400×10⁴/mL, 6.2% and 2.6%; (B): 420×10⁴/mL, 44% and 4.6%; (C): 660×10⁴/mL, 1.8% and 0.8%.

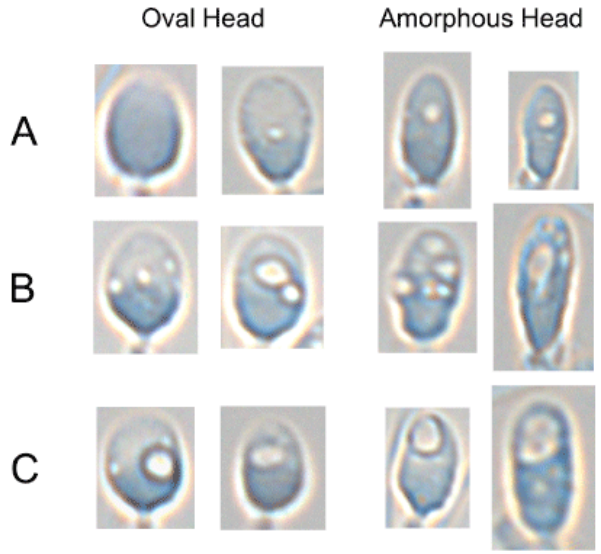

Figure 5: Classification of vacuoles on the basis of the number and size (A): novacuoleor one small vacuole, (B): multiple sporadic vacuoles, and (C): one large vacuole.

at 630X magnification under common bright field microscope, small-sized vacuole was clearly recognized in the images (Figures 1-5).

Berkovitz et al. suggested that microinjection of sperm with normal morphology but containing a large vacuole affected the pregnancy outcome, resulted in significantly lower rates of pregnancy and higher rates of spontaneous abortion [11,12]. Anetiological correlation between vacuole and DNA fragmentation due to Double Strand Break (DSB) is often put forth in the literature as an explanation to these clinical outcomes. Franco et al. suggested that Large Nuclear Vacuoles (LNV) that occupy more than 50% of the nuclear area might be relevant for some molecular anomalies such as abnormal chromatin packaging, which facilitates DNA damage [28,29]. They also proposed that rejection of the sperm with LNV by MSOME might therefore result in improved outcomes. Conventional ICSI equipment readily recognizes LNV possibly of those in group C (Figure 5), but not sperm with smaller vacuoles characteristic of groups A and B. However, they did not refer to smaller vacuoles in their study [28,29].

The present results revealed important issue in clinical ART: a variety of vacuoles were involved in human sperm regardless of the normality of outline or their motility, and that DNA might be absent or to be present at low density in them. We also revealed that the commonly used processing method that employed in the present study could not isolate motile sperm without vacuoles. The repair of DSB is intrinsically difficult compared with that of other DNA lesions, and the critical threshold of DNA fragmentation may be extremely low [30,31]. We developed the single-cell pulsed-field gel electrophoresis to visualize the early stage of DNA fragmentation [32,33]. We observed that even after separating motile sperm through the same procedures in the present study, some of motile sperm have undergone an early stage of DNA fragmentation, the frequency of which varied among ejaculates. These two results suggest that motility could not offer complete assurance in terms of the vacuole and DNA integrity. It is necessary to determine whether the vacuoles found in the motile sperm are responsible for DNA fragmentation, and whether they wholly or partly constitute the damage. It is also necessary to investigate whether their sizes correlate with the degree of damage. We have a simple question of whether the early stage of DNA fragmentation caused some morphological alterations that could be recognized via light microscopy. Thus, we intend to develop a method for simultaneous determination of the vacuole and DNA damage in a single sperm.

For the specimens shown in Figure 4, it would be difficult to determine the appropriate sperm for IMSI through intraoperative one-by-one MSOME observation. A novel translucent staining for simultaneous visualization of the outline and vacuoles constitutes a major step for pre-ART cyto-diagnosis to determine whether the sperm population is competent for use in clinical ICSI. In contrast, MSOME deals with the intra-operative final confirmation for motile sperm that will be actually injected.

References

1. Palermo G, Joris H, Devroey P, Van Steirteghem AC (1992) Pregnancies after intracytoplasmic injection of single spermatozoon into an oocyte. Lancet 340: 17-18.
2. Aitken RJ, De Iuliis GN (2007) Origins and consequences of DNA damage in male germ cells. Reprod Biomed Online 14: 727-733.
3. Aitken RJ, De Iuliis GN (2007) Value of DNA integrity assays for fertility evaluation. Soc Reprod Fertil Suppl 65: 81-92.
4. Simon L, Brunborg G, Stevenson M, Lutton D, McManus J, et al. (2010) Clinical significance of sperm DNA damage in assisted reproduction outcome. Hum Reprod 25: 1594-1608.
5. Irvine DS, Twigg JP, Gordon EL, Fulton N, Milne PA, et al. (2000) DNA integrity in human spermatozoa: relationships with semen quality. J Androl 21: 33-44.
6. Green NS (2004) Risks of birth defects and other adverse outcomes associated with assisted reproductive technology. Pediatrics 114: 256-259.
7. Zini A, Boman JM, Belzile E, Ciampi A (2008) Sperm DNA damage is associated with an increased risk of pregnancy loss after IVF and ICSI: systematic review and meta-analysis. Hum Reprod 23: 2663-2668.
8. Davies MJ, Moore VM, Willson KJ, Van Essen P, Priest K, et al. (2012) Reproductive technologies and the risk of birth defects. N Engl J Med 366: 1803-1813.
9. E. Moretti E, Collodel G (2012) Electron microscopy in the study of human sperm pathologies. In Current microscopy contributions to advances in science and technology. (Méndez-Vilas A Edn), Formatex Research Center, Badajoz, Spain, pp- 343-351.

10. Bartoov B, Berkovitz A, Eltes F, Kogosovsky A, Yagoda A, et al. (2003) Pregnancy rates are higher with intracytoplasmic morphologically selected sperm injection than with conventional intracytoplasmic injection. Fertil Steril 80: 1413-1419.

11. Berkovitz A, Eltes F, Yaari S, Katz N, Barr I, et al. (2005) The morphological normalcy of the sperm nucleus and pregnancy rate of intracytoplasmic injection with morphologically selected sperm. Hum Reprod 20: 185-190.

12. Berkovitz A, Eltes F, Ellenbogen A, Peer S, Feldberg D, et al. (2006) Does the presence of nuclear vacuoles in human sperm selected for ICSI affect pregnancy outcome? Hum Reprod 21: 1787-1790.

13. Knez K, Tomazevic T, Zorn B, Vrtacnik-Bokal E, Virant-Klun I (2012) Intracytoplasmic morphologically selected sperm injection improves development and quality of preimplantation embryos in teratozoospermia patients. Reprod Biomed Online 25: 168-179.

14. Antinori M, Licata E, Dani G, Cerusico F, Versaci C, et al. (2008) Intracytoplasmic morphologically selected sperm injection: a prospective randomized trial. Reprod Biomed Online 16: 835-841.

15. Rice WR, Singleton FM (1989) Reactive blue 2 selectively inhibits P2y-purinoceptor-stimulated surfactant phospholipid secretion from rat isolated alveolar type II cells. Br J Pharmacol 97: 158-162.

16. Kennedy C (1990) P1- and P2-purinoceptor subtypes--an update. Arch Int Pharmacodyn Ther 303: 30-50.

17. Subramanian S (1984) Dye-ligand affinity chromatography: the interaction of Cibacron Blue F3GA with proteins and enzymes. CRC Crit Rev Biochem 16: 169-205.

18. Leatherbarrow RJ, Dean PD (1980) Studies on the mechanism of binding of serum albumins to immobilized cibacron blue F3G A. Biochem J 189: 27-34.

19. Bohácová V, Docolomanský P, Breier A, Gemeiner P, Ziegelhöffer A (1998) Interaction of lactate dehydrogenase with anthraquinone dyes: characterization of ligands for dye-ligand chromatography. J Chromatogr B Biomed Sci Appl 715: 273-281.

20. La Vignera S, Condorelli RA, Vicari E, D'Agata R, Salemi M, et al. (2012) High levels of lipid peroxidation in semen of diabetic patients. Andrologia 44 Suppl 1: 565-570.

21. Kaneko S, Oshio S, Kobanawa K, Kobayashi T, Mohri H, et al. (1986) Purification of human sperm by a discontinuous Percoll density gradient with an innercolumn. Biol Reprod 35: 1059-1063.

22. Kaneko S, Sato H, Kobanawa K, Oshio S, Kobayashi T, et al. (1987) Continuous-step density gradient centrifugation for the selective concentration of progressively motile sperm for insemination with husband's semen. Arch Androl 19: 75-84.

23. Kruger TF, Ackerman SB, Simmons KF, Swanson RJ, Brugo SS, et al. (1987) A quick, reliable staining technique for human sperm morphology. Arch Androl 18: 275-277.

24. Kuroda Y, Kaneko S, Matsuda Y, Akihama S, Nozawa S (1996) Selective isolation of acrosome reacted human sperm with progressive motility by using cell affinity chromatography on concanavalin A Sepharose. Andrologia 28: 7-13.

25. Kruger TF, Acosta AA, Simmons KF, Swanson RJ, Matta JF, et al. (1988) Predictive value of abnormal sperm morphology in *in vitro* fertilization. Fertil Steril 49: 112-117.

26. Schulte EK (1991) Standardization of biological dyes and stains: pitfalls and possibilities. Histochemistry 95: 319-328.

27. Kruger TF, du Toit TC, Franken DR, Menkveld R, Lombard CJ (1995) Sperm morphology: assessing the agreement between the manual method (strict criteria) and the sperm morphology analyzer IVOS. Fertil Steril 63: 134-141.

28. Franco JG Jr, Baruffi RL, Mauri AL, Petersen CG, Oliveira JB, et al. (2008) Significance of large nuclear vacuoles in human spermatozoa: implications for ICSI. Reprod Biomed Online 17: 42-45.

29. Franco JG Jr, Mauri AL, Petersen CG, Massaro FC, Silva LF, et al. (2012) Large nuclear vacuoles are indicative of abnormal chromatin packaging in human spermatozoa. Int J Androl 35: 46-51.

30. Khanna KK, Jackson SP (2001) DNA double-strand breaks: signaling, repair and the cancer connection. Nat Genet 27: 247-254.

31. Hefferin ML, Tomkinson AE (2005) Mechanism of DNA double-strand break repair by non-homologous end joining. DNA Repair (Amst) 4: 639-648.

32. Kaneko S, Yoshida J, Ishikawa H, Takamatsu K (2012) Single-cell pulsed-field gel electrophoresis to detect the early stage of DNA fragmentation in human sperm nuclei. PLoS One 7: e42257.

33. Kaneko S, Yoshida J, Ishikawa H, Takamatsu K (2013) Single-Nuclear DNA Instability Analyses by Means of Single-Cell Pulsed Field Gel Electrophoresis - Technical Problems of the Comet Assay and Their Solutions for Quantitative Measurements. J Mol Biomark Diagn S5-005.